Electronic structure of substoichiometric carbides and nitrides of titanium and vanadium

P. Marksteiner and P. Weinberger
Institut für Technische Elektrochemie, Technische Universität Wien, Getreidemarkt 9, A-1060 Wien, Austria

A. Neckel
Institut für Physikalische Chemie, Technische Universität Wien, Währingerstrasse 42, A-1090 Wien, Austria

R. Zeller and P. H. Dederichs
Institut für Festkörperforschung der Kernforschungsanlage Jülich, Postfach 1913, D-5170 Jülich, Federal Republic of Germany

(Received 24 June 1985)

The Korringa-Kohn-Rostoker—coherent-potential-approximation (KKR-CPA) and the Korringa-Kohn-Rostoker—Green's-function (KKR-GF) methods are applied to study the electronic structure of substoichiometric TiC_x, TiN_x, VC_x, and VN_x. The introduction of vacancies in the nonmetal sublattice influences the electronic structure of all these compounds in a similar way: an additional sharp "vacancy peak" appears in the density of states, which, with increasing vacancy concentration, is broadened and shifted to higher energies. The Fermi energy is generally lowered by the introduction of vacancies.

I. INTRODUCTION

The electronic structure of stoichiometric refractory metal compounds MX (M=Ti,V,Zr,Nb,Ta,Hf; X=C,N,O), which crystallize in the rocksalt structure, has been extensively studied during the past 20 years (see, for instance, the review article by Neckel[1]). However, all of these compounds show large deviations from stoichiometry, and stoichiometric samples, if any, can only be obtained with great difficulty. Experimental evidence shows that there can be large amounts of vacancies on the nonmetal sublattice, while the metal sublattice remains fully occupied. Only in a few cases with high nonmetal content have metal vacancies been observed.

Various theoretical attempts have been made to account for the vacancies.[2–7] One fundamental problem is the proper description of the ordering of the vacancies. The case of a completely ordered superstructure can be treated by standard band-structure methods, whereas the theory of random alloys can be applied to a completely disordered nonmetal sublattice. The problem of short-range order involves the calculation of non-site-diagonal Green's functions and has been—up to now—only theoretically discussed. In the compounds studied in this work several superstructures have been observed: V_6C_5, V_8C_7, Ti_2C, Ti_2N, $V_{16}N_{13}$ (Landesman[8] and references therein). Various degrees of short-range order have been observed by diffuse neutron scattering (Moisy-Maurice *et al.*,[9] Sauvage *et al.*[10]).

The KKR-CPA method we use in this work treats the case of completely randomly arranged vacancies and is justified by the following reasons.

(1) Notwithstanding the existence of ordered compounds obtained by annealing, quenching yields samples with little or no order over a wide range of concentrations. Moreover, in the "ordered compounds," such as $V_6C_5\square$ ($\square$ denoting a carbon vacancy) the occupancy of the carbon sites is not equal to one, and the occupancy of the vacancy sites is not equal to zero.

(2) The results of the CPA calculations can be used as a basis for the calculation of short-range order effects by embedding a cluster in the CPA medium. We intend to do this in the near future, including also the effects of lattice distortions around the vacancies.

We have performed several calculations on the compounds TiC_x, TiN_x, VC_x, and VN_x. The range of concentrations x was chosen such that the whole range of existence of these compounds is covered.

II. THEORETICAL ASPECTS

Since we follow closely the formalism described by Klima *et al.*,[7] we refer the reader to this paper for details; here we give only a short summary.

The central problem of the constant energy mode Korringa-Kohn-Rostoker method is the calculation of the cell-diagonal scattering path operator $\underset{\sim}{\tau}^{00}$ corresponding to an ordered lattice of (effective) scatterers. Since the NaCl lattice consists of two fcc sublattices, the scattering path operator is conveniently written as a 2×2 supermatrix $\underset{\sim}{\tau}^{00}$ with elements $\underset{\sim}{\tau}^{00}_{ss'}$, the indices s and s' denoting the respective sublattices,

$$\underset{\sim}{\tau}^{00}(E)=\frac{1}{\Omega_{BZ}}\int_{BZ}[\underset{\sim}{t}(E)^{-1}-\underset{\sim}{G}(E,\mathbf{k})]^{-1}d^3k \ . \qquad (1)$$

In Eq. (1) E is the energy, Ω_{BZ} is the volume of the Brillouin zone, and $\underset{\sim}{G}(E,\mathbf{k})$ are the KKR structure constants (Stocks *et al.*[11]). In the following the obvious parameter E will be dropped. $\underset{\sim}{t}$ is a diagonal supermatrix with diagonal elements $\underline{t}_{ss}$. If both sublattices are stoichiometric, $\underline{t}_{ss}$ is equal to the single-site t-matrix $\underline{t}^{\alpha}$, corresponding to atoms of species α placed on sublattice s. The matrix

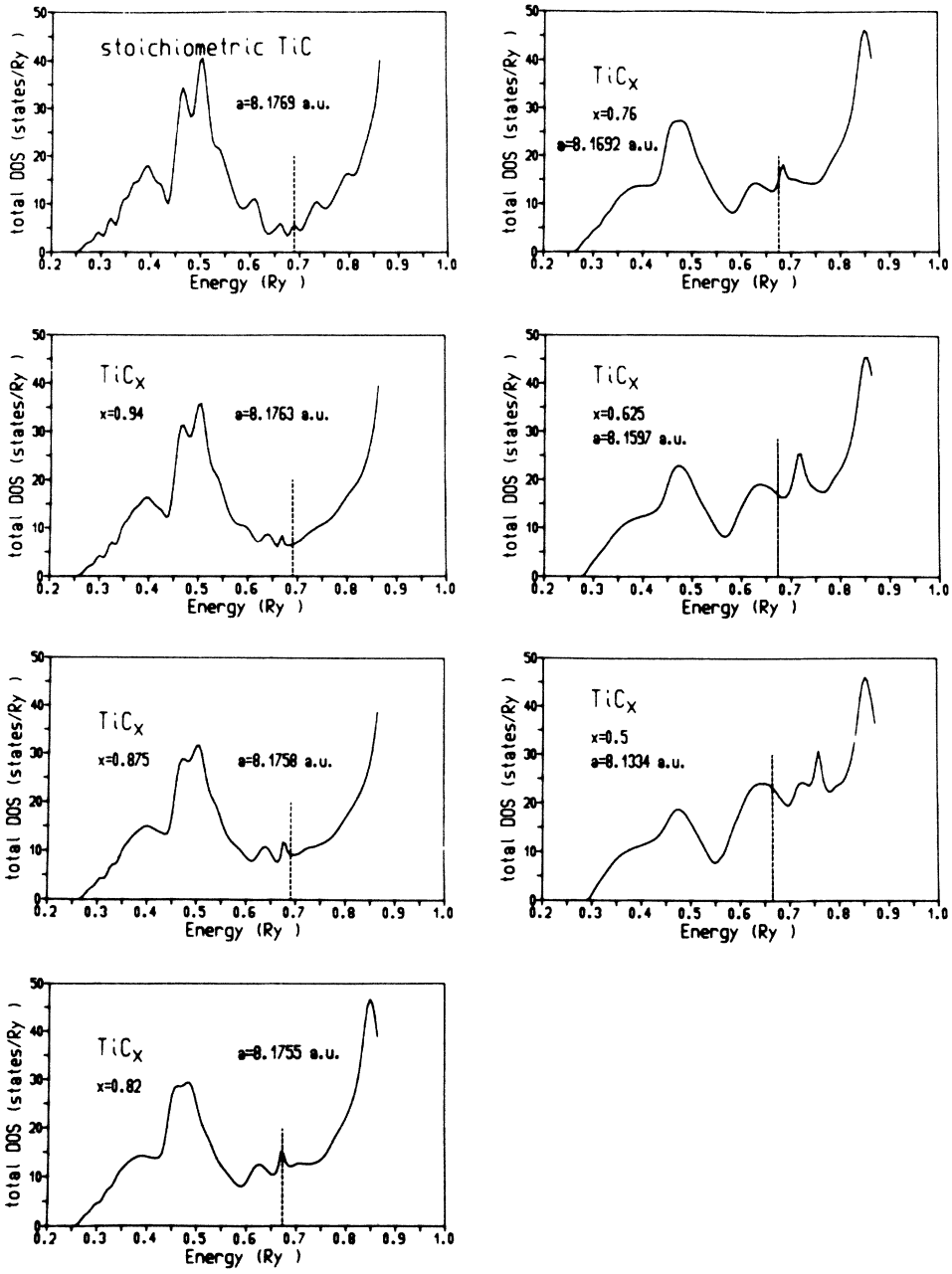

FIG. 1. Total density of states for TiC_x, concentration and lattice parameter are indicated in each case.

elements $t^{\alpha}_{ll'}$ are calculated from the scattering phase shifts η^{α}_{l} by

$$t^{\alpha}_{ll'} = -\frac{1}{\sqrt{E}} (\sin\eta^{\alpha}_{l}) \exp(i\eta^{\alpha}_{l})\delta_{ll'} . \tag{2}$$

If only the second sublattice is stoichiometric and the first is disordered, $\underline{t}_{11}$ is equal to the effective t minus matrix $\underline{t}^{c}$ given by the CPA condition

$$c_A \underline{M}^{A} \underline{D}_1^{A,00} + (1-c_A)\underline{M}^{B} \underline{D}_1^{B,00} = \underline{0} , \tag{3}$$

where

$$\underline{M}^{\alpha} = (\underline{t}^{\alpha})^{-1} - (\underline{t}^{c})^{-1}, \tag{4}$$

$$\underline{D}_1^{\alpha,00} = (\underline{1} + \underline{\tau}_{11}^{00} \underline{M}^{\alpha})^{-1} . \tag{5}$$

c_A is the concentration of species A on sublattice 1, and α stands for species A or B. Equations (1) and (3) have to be solved self-consistently.

The total density of states is the sum of contributions $g_1(E)$ and $g_2(E)$ of the two sublattices, the former can be further decomposed into component densities of states,

$$g(E) = c_A g_1^{A}(E) + (1-c_A) g_1^{B}(E) + g_2^{X}(E) , \tag{6}$$

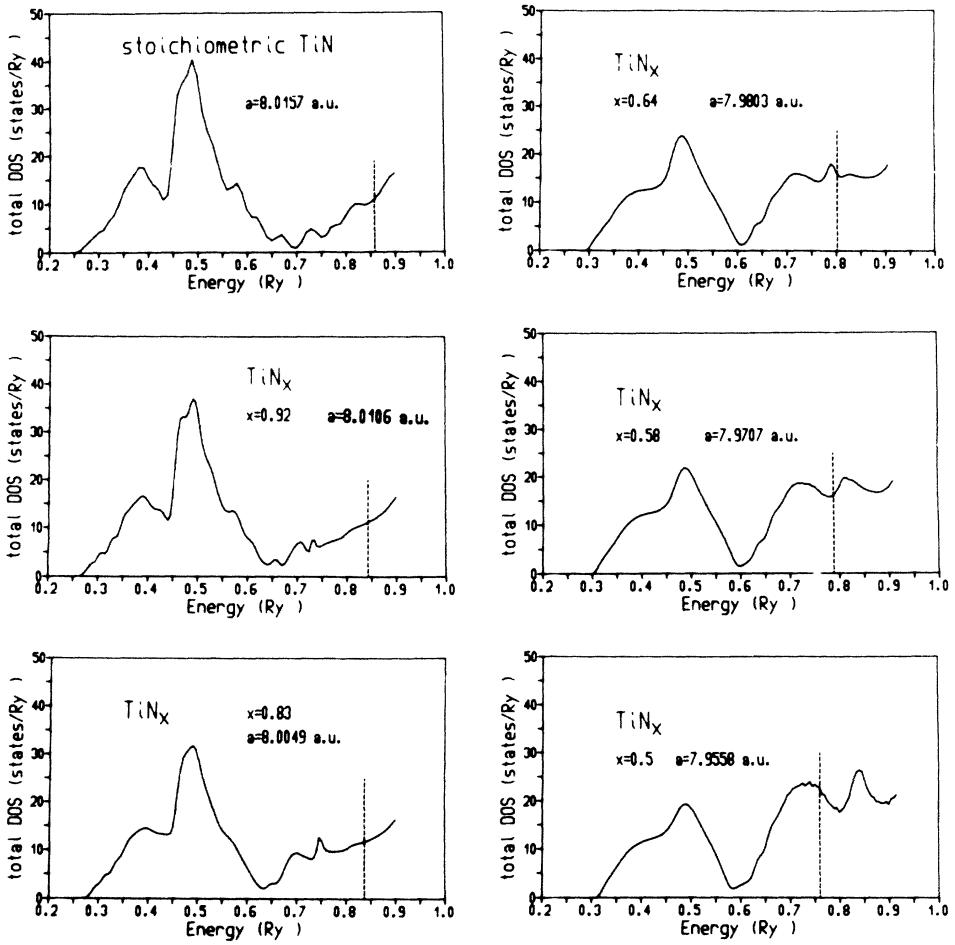

FIG. 2. Total density of states for TiN_x, concentration and lattice parameter are indicated in each case.

X denoting the species on sublattice 2.

The partial densities of states are defined as

$$g_1^{\alpha}(E) = -\frac{1}{\pi} \operatorname{Im} \operatorname{tr} \left[\underline{D}_1^{\alpha,00} \underline{\tau}_{11}^{00} \int_{\Omega_1} Z_L^{\alpha}(E,\mathbf{r}) Z_{L'}^{\alpha}(E,\mathbf{r}) d^3r \right], \tag{7}$$

$$g_2^{X}(E) = -\frac{1}{\pi} \operatorname{Im} \operatorname{tr} \left[\underline{\tau}_{22}^{00} \int_{\Omega_2} Z_L^{X}(E,\mathbf{r}) Z_{L'}^{X}(E,\mathbf{r}) d^3r \right], \tag{8}$$

where $Z_L^{\alpha}(E,\mathbf{r})$ are solutions of the Schrödinger equation corresponding to the muffin-tin potential of species α and are normalized to single-site scattering (Faulkner[12]).

III. COMPUTATIONAL DETAILS

The phase shifts for the metal and nonmetal atoms were calculated from self-consistent APW potentials by Neckel *et al.*[13] The self-consistent APW potentials of the vacancy sphere in the ordered defect structure $Ti_3^{[4]}Ti^{[6]}X_3\square$ (X=C,N,□= vacancy, the numbers in square brackets denote the respective coordination numbers) by Redinger *et al.*[6] and Herzig *et al.*[14] were used to calculate the vacancy phase shifts for TiC_x and TiN_x. For the vanadium compounds no such calculations are available. Therefore we calculated the charge densities of free $V^{0.75+}$ and X^- atoms using the $X\alpha$ approximation, the anions being stabilized by Watson spheres.[15] The vacancy potential was obtained by a superposition of these charge densities on the corresponding lattice sites of the ordered defect structure mentioned above. The vacancy potentials in all these compounds look very much the same, all having a flat maximum of about 0.5 Ry above the muffin-tin zero (see also the discussion by Klima *et al.*[7]).

In the case of TiC_x ($x \leq 0.82$) we used the potential of the defect structure also for the calculation of the Ti and C phase shifts. Since there are two different Ti sites in this structure with two different potentials, the weighted average over these was taken. For TiC_x ($x \geq 0.875$) we used the Ti and C self-consistent APW potentials of stoichiometric TiC. Since for TiC_x the use of different potentials gives rise to a slight inconsistency regarding the

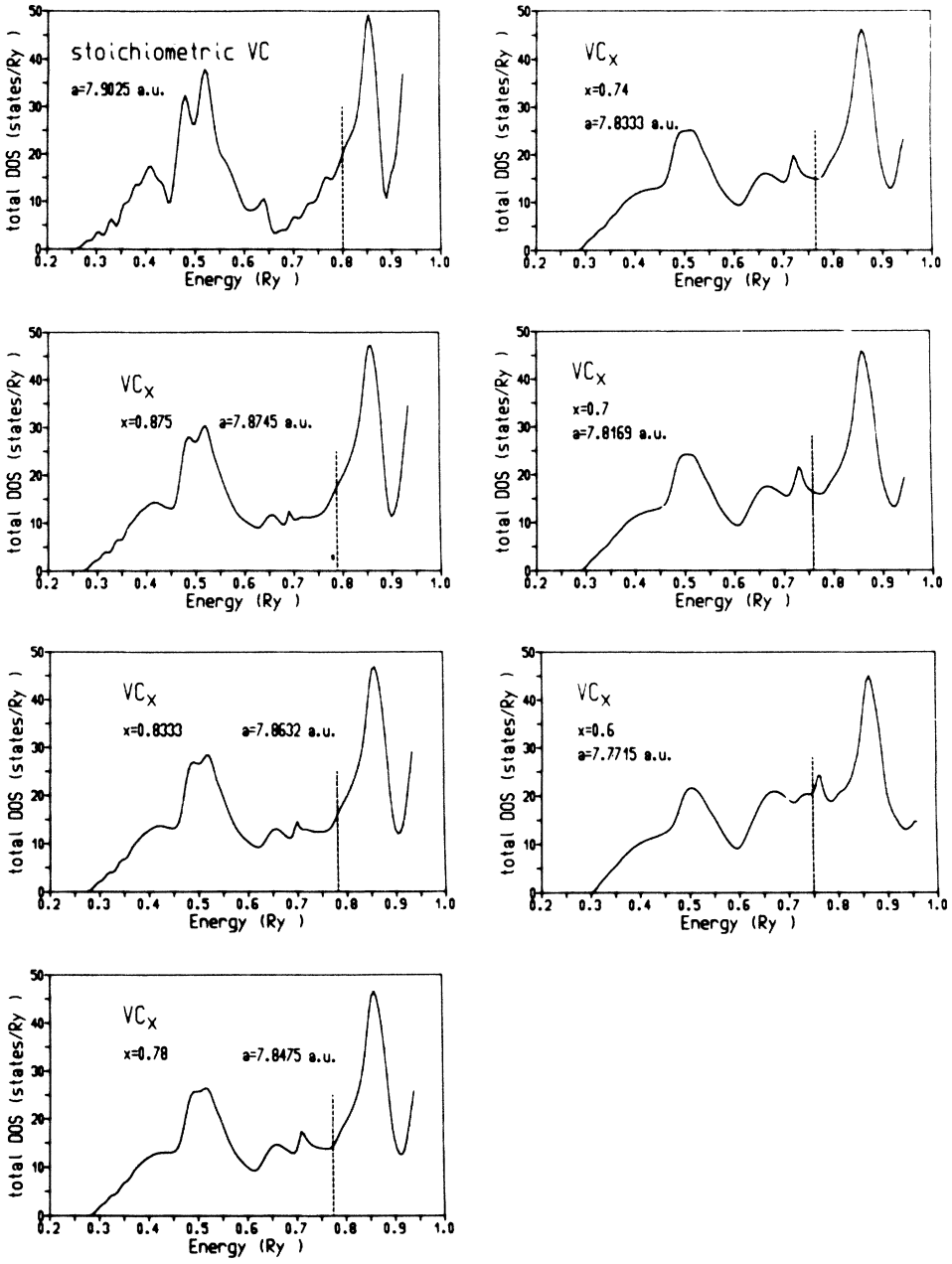

FIG. 3. Total density of states for VC_x, concentration and lattice parameter are indicated in each case.

zero of the energy scale, for TiN_x we used the potential of stoichiometric TiN for the whole range of concentrations. The influence of the choice of potential on the results will be discussed in Sec. IV.

The data available on the lattice constants of substoichiometric refractory carbides and nitrides are scant and by no means consistent. For TiC_x and VC_x we used chiefly the values given by Rudy,[16] for TiN_x those by Nørlund Christensen and Fregerslev,[17] and for VN_x those by Brauer and Schnell.[18] Some values given by Landesman,[8] as well as those used by Neckel *et al.*[13] and by Redinger *et al.*[6] were also taken into account.

The Brillouin-zone integral in Eq. (1) was performed by the special directions method of Bansil.[19] Generally the 21 directions given by Fehlner and Vosko[20] were used, whereby the KKR matrix was evaluated at about 100–250 points along each direction. Scattering amplitudes and scattering path operators were calculated at an energy grid of 0.005 Ry using complex energies to avoid the singularities of the integrand at the real energy axis. The imaginary part of the energy was chosen between 0.015 and 0.02 Ry. Using extrapolation of the scattering amplitudes, one or two iterations were sufficient to reach convergence with respect to the CPA condition. Scatter-

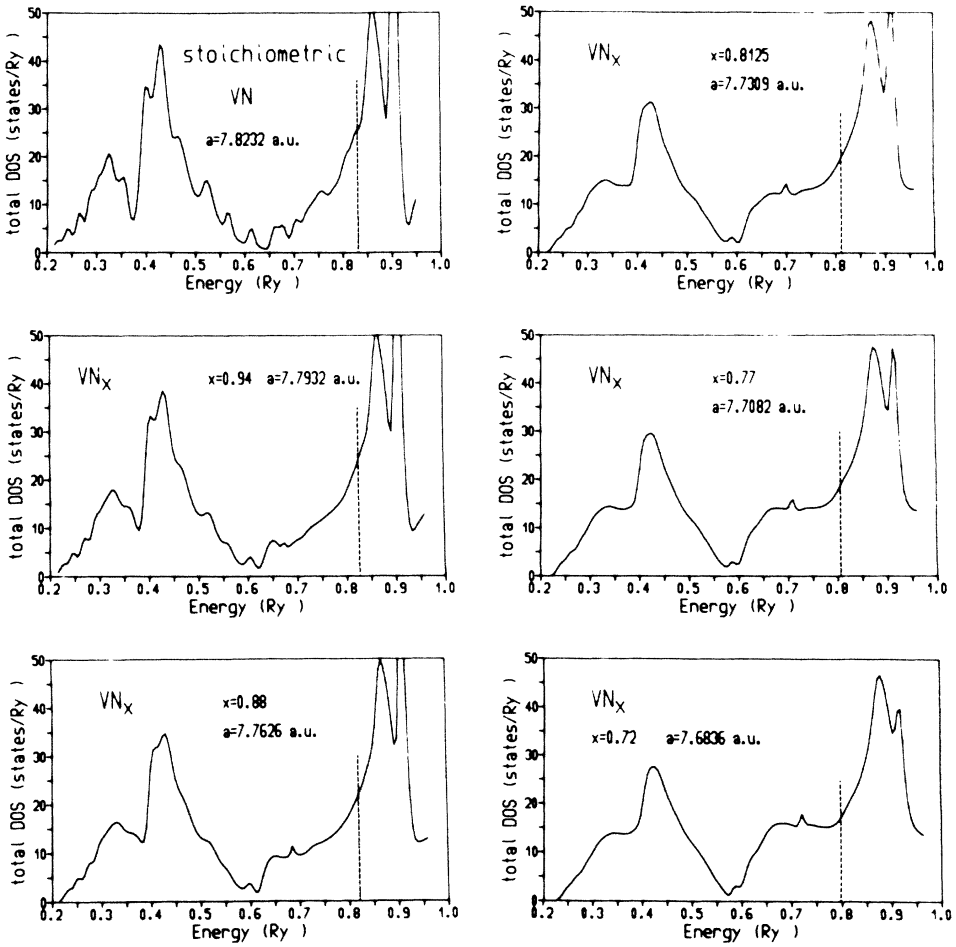

FIG. 4. Total density of states for VN_x, concentration and lattice parameter are indicated in each case.

ing amplitudes and scattering path operators were then analytically continued to the real axis by means of the Cauchy-Riemann condition.

IV. RESULTS

The total densities of states (DOS) of TiC_x, TiN_x, VC_x, and VN_x for various concentrations x are shown in Figs. 1–4. The Fermi energy is shown as a dashed line. For convenience these figures are labeled by the respective concentrations x and lattice constants a.

Figures 5–8 show the main contributions to the local partial densities of states. In the left-hand column the solid line corresponds to the metal t_{2g} DOS, the dotted line to the metal e_g DOS. The center column shows the nonmetal t_{1u} (p-like) DOS, the right-hand column the vacancy a_{1g} (s-like, solid line) DOS, and t_{1u} (p-like, dotted line) DOS. All other contributions to the DOS which are not shown in Figs. 5–8 are very small.

Some general trends are common to all these compounds.

(1) With increasing vacancy concentration the DOS becomes less structured and all sharp peaks are smoothed.

(2) The peaks chiefly made up by nonmetal p-electrons ("nonmetal peaks") lose intensity. This is not surprising, since there are fewer nonmetal electrons present. However, it is not *a priori* self-evident, since the loss of electrons might conceivably be accounted for by lowering the Fermi energy.

(3) The peaks above the Fermi energy with mainly metal d character ("metal peaks") are little affected by the introduction of vacancies.

(4) The most striking feature is the appearance of additional peaks ("vacancy peaks") near the minimum of the DOS of the stoichiometric compounds. For small vacancy concentrations there appears a shoulder which, with increasing vacancy concentration, splits off into a separate somewhat diffuse peak.

As regards the position of the peaks, the nonmetal peaks are not affected at all by the vacancies. The sharp vacancy peaks are constantly shifted to higher energies, the overall energy difference between the stoichiometric case and the case with highest vacancy concentration

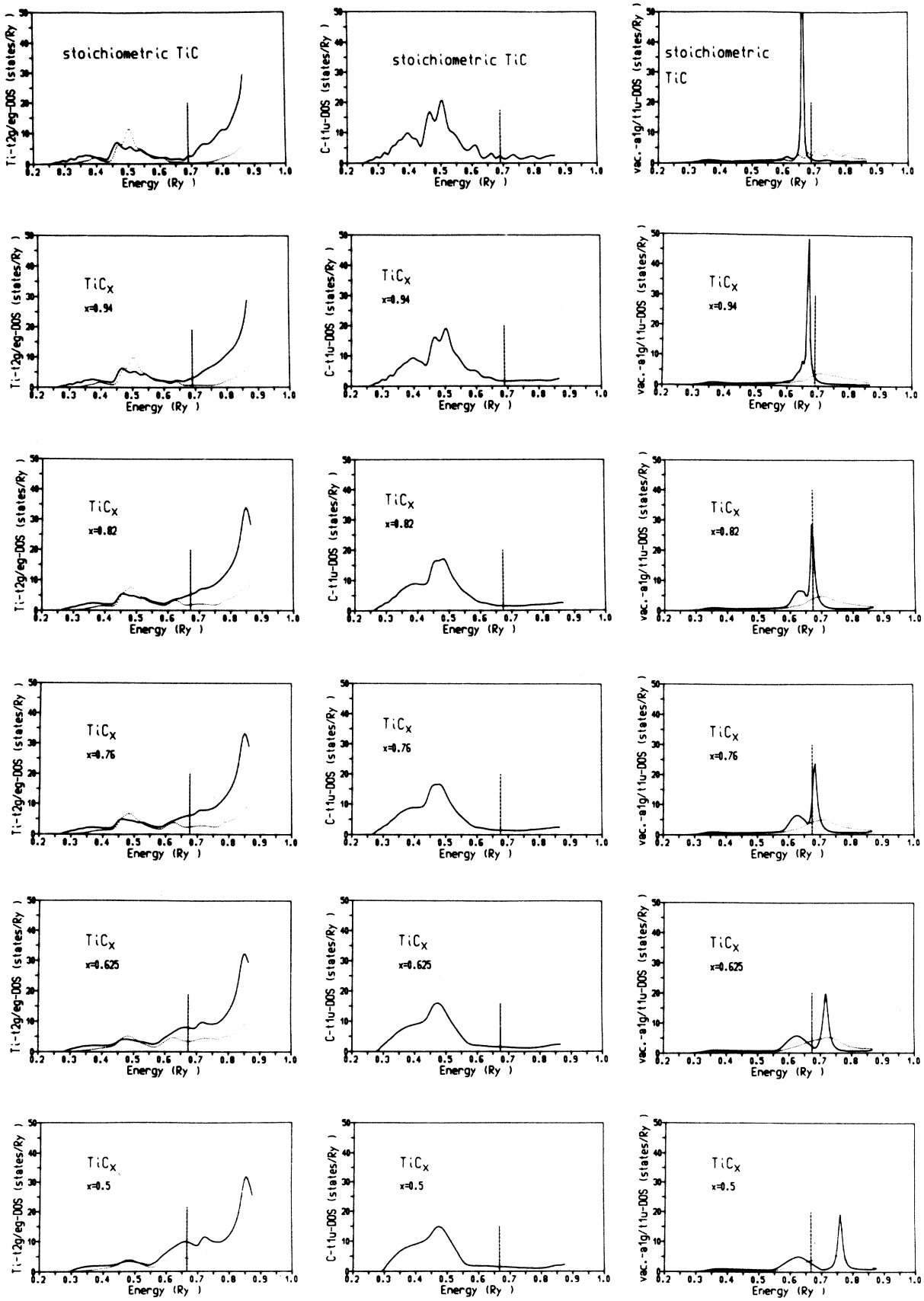

FIG. 5. Partial densities of states for TiC_x. Left column, t_{2g}- (solid line) and e_g- (dotted line) like metal partial DOS; center column, t_{1u}-like nonmetal partial DOS; right column, a_{1g}- (solid line) and t_{1u}- (dotted line) like vacancy partial DOS.

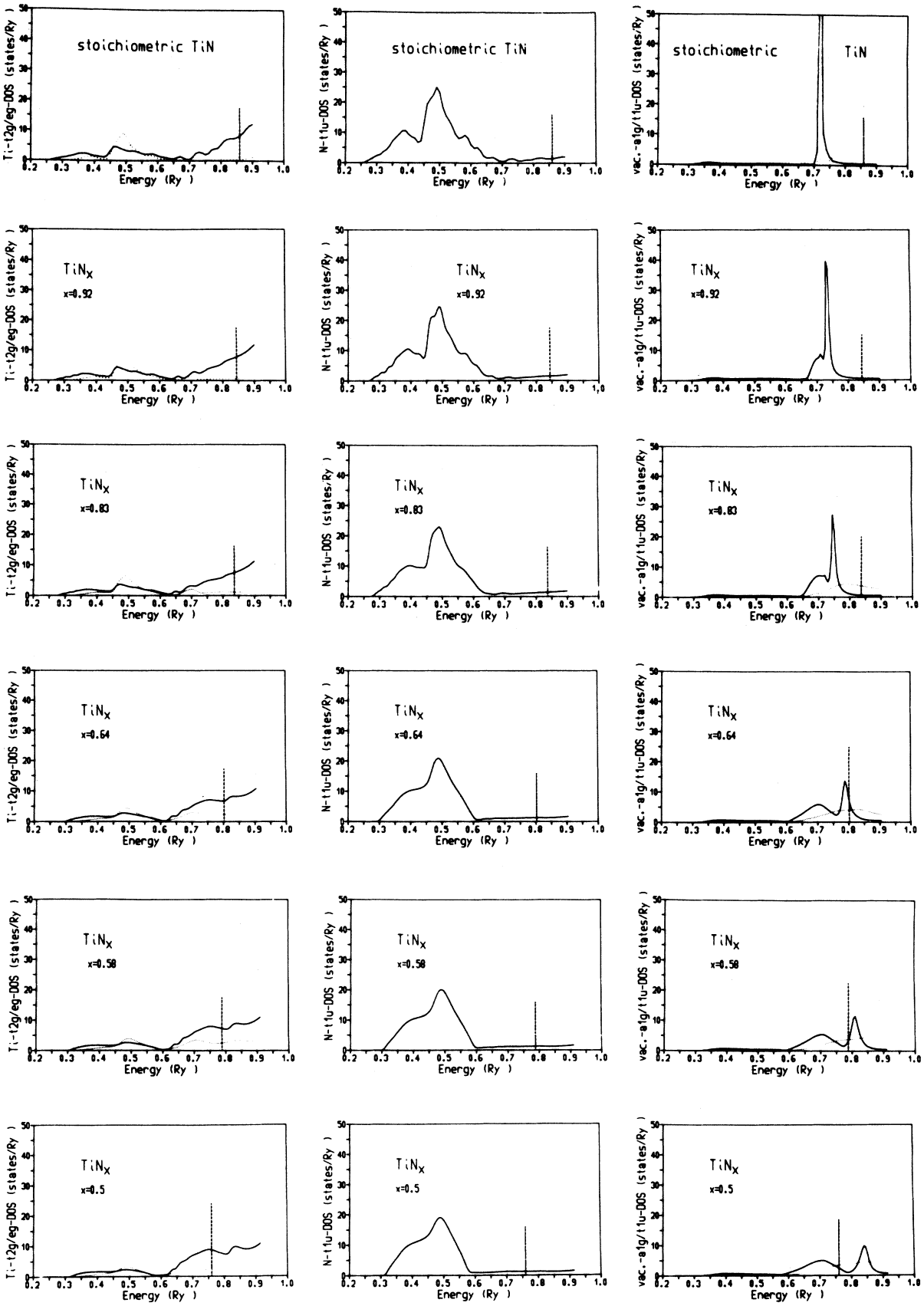

FIG. 6. Partial densities of states for TiN_x. Left column, t_{2g}- (solid line) and e_g- (dotted line) like metal partial DOS; center column, t_{1u}-like nonmetal partial DOS; right column, a_{1g}- (solid line) and t_{1u}- (dotted line) like vacancy partial DOS.

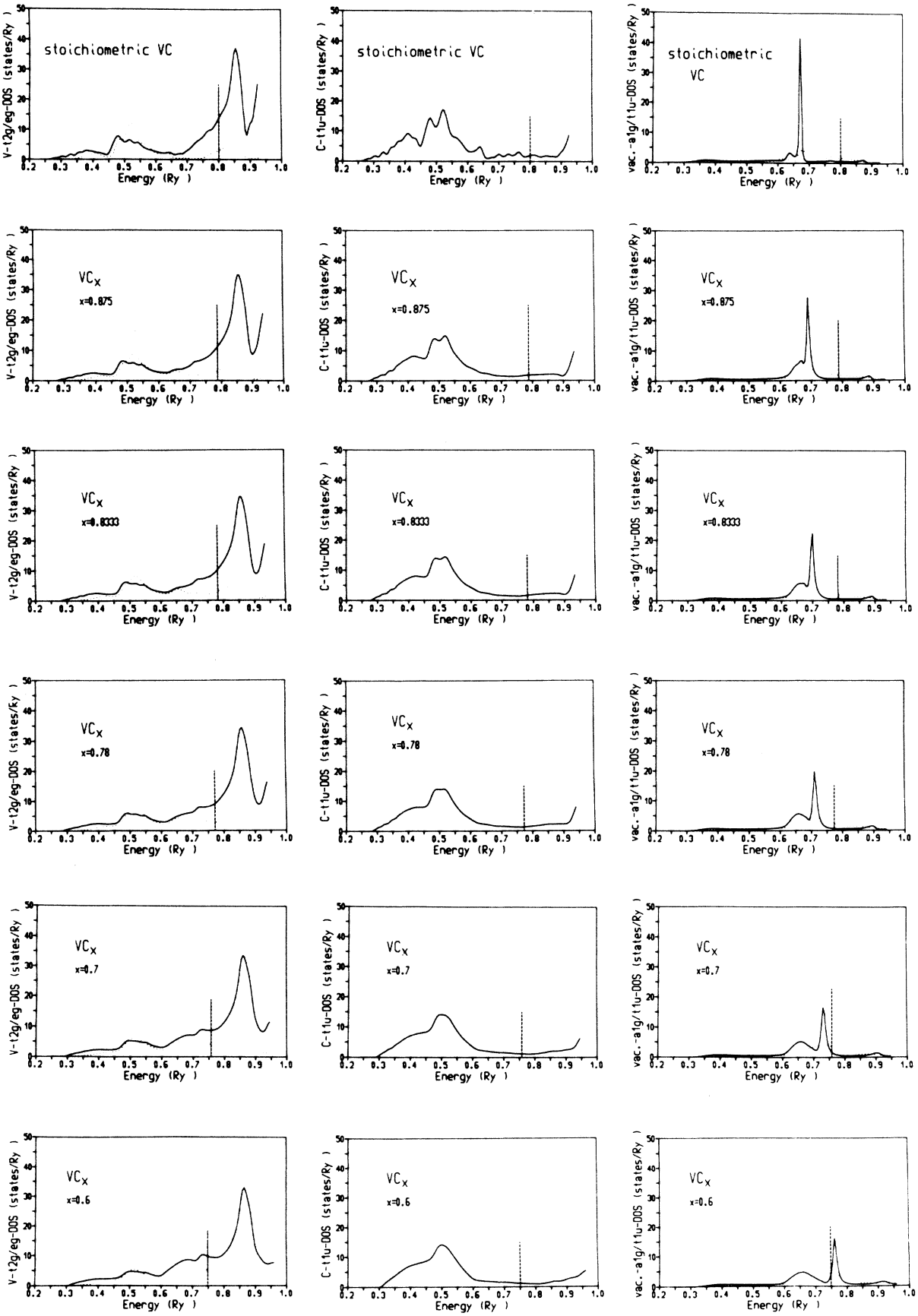

FIG. 7. Partial densities of states for VC_x. Left column, t_{2g}- (solid line) and e_g- (dotted line) like metal partial DOS; center column, t_{1u}-like nonmetal partial DOS; right column, a_{1g}- (solid line) and t_{1u}- (dotted line) like vacancy partial DOS.

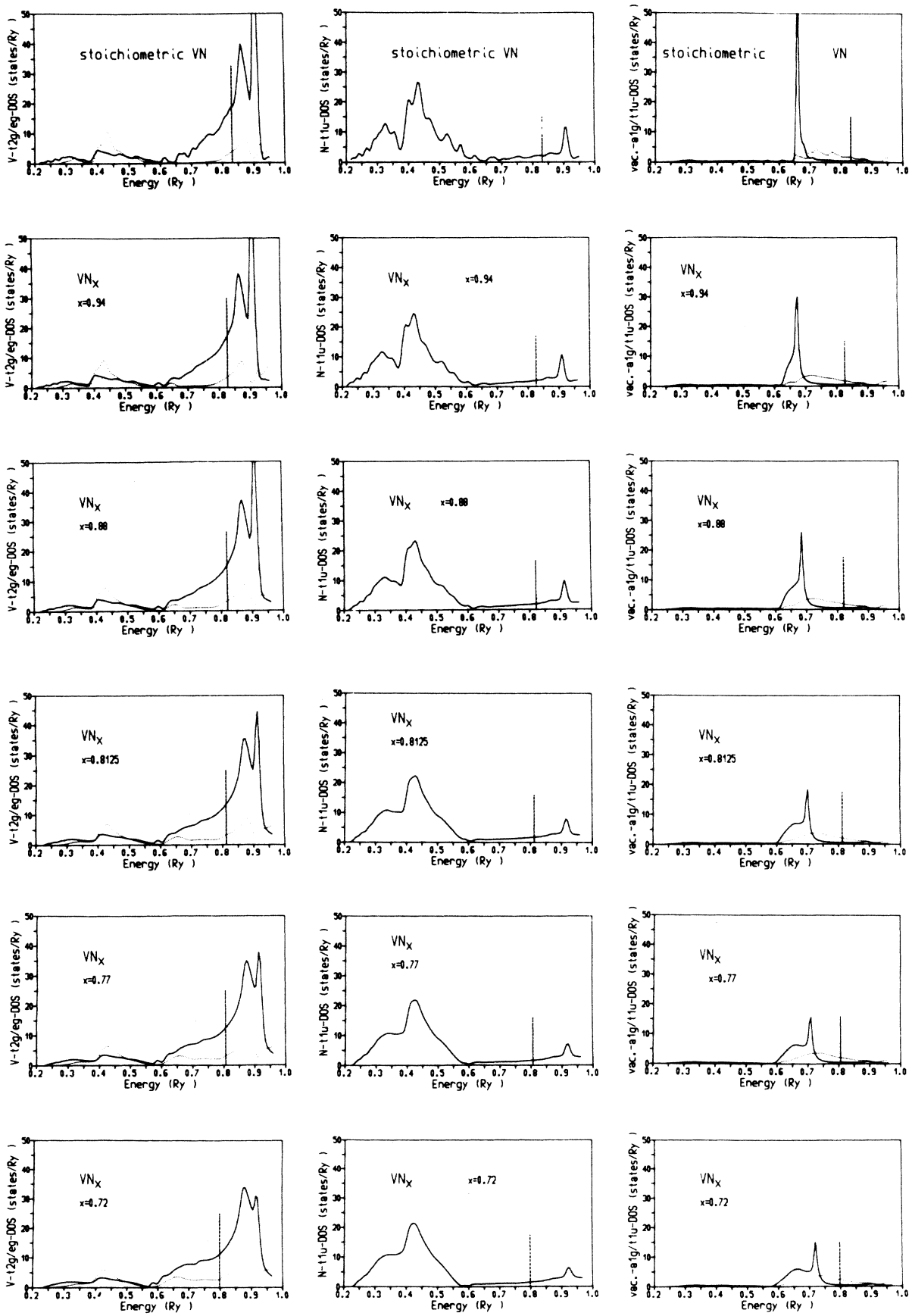

FIG. 8. Partial densities of states for VN_x. Left column, t_{2g}- (full line) and e_g- (dotted line) like metal partial DOS; center column, t_{1u}-like nonmetal partial DOS; right column, a_{1g}- (full line) and t_{1u}- (dotted line) like vacancy partial DOS.

amounting to about 0.1 Ry. The diffuse split-off vacancy peaks remain nearly unchanged in energy.

In the case of TiC_x there seems to be an exception to these general trends: going from $TiC_{0.94}$ to $TiC_{0.82}$ the nonmetal peaks are shifted to lower energies by 0.02 Ry, and the vacancy peak is not shifted at all (with respect to $TiC_{0.875}$—which is not included in Figs. 1 and 5—the vacancy peak is even lowered). Also, there is a sharp drop in the Fermi energy of nearly 0.02 Ry going from $TiC_{0.875}$ to $TiC_{0.82}$, whereas the Fermi energy is the same for $TiC_{1.0}$, $TiC_{0.94}$, and $TiC_{0.875}$ (see Fig. 9). Here one must bear in mind that, as was already mentioned in Sec. III, two different potentials are used. All these inconsistencies are resolved if one chooses the zero of the energy scale—which is arbitrary—about 0.02 Ry lower for all the cases where the potential of the APW-$Ti_4C_3\square$ calculation is used. Then all the peaks fit perfectly into the trends mentioned above. The only noticeable effect of the use of different potentials is then the position of the metal peak, which differs by about 0.01 Ry—a very insignificant difference indeed.

This indicates that the choice of the potential should not be too crucial. Although a CPA calculation carried out to self-consistency with respect to the charge density would remove all ambiguities concerning the potential, the additional computational effort does not seem worthwhile.

The density of states at the Fermi energy is of special interest since it can be—with neglect of electron-phonon enhancement—directly compared with experimentally determined values of the linear coefficient of the specific heat. The Fermi energy itself and the density of states at the Fermi energy are plotted versus the nonmetal concentration in Figs. 9–12.

With increasing vacancy concentration the Fermi energy is generally lowered. Since the slope of the density is, except for TiC, positive in the vicinity of the Fermi level in the stoichiometric compounds, the density of states at the Fermi energy can be expected to be lowered also. This is in fact the case for all concentrations of VN_x and for VC_x with less than 20% vacancies. If, however, the Fermi energy passes through the vacancy peak, the density of states at the Fermi energy rises again.

Because of the incompatibility of the potentials used, for TiC_x there is an artificial bump in the curve for the Fermi energy. The value of the density of states at the Fermi energy is, of course, not affected by this artifact.

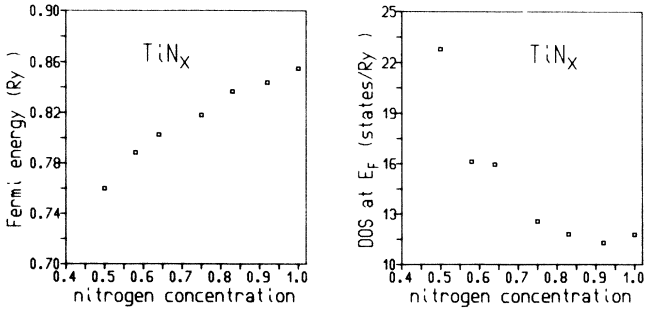

FIG. 10. Fermi energy and density of states at the Fermi energy for TiN_x versus concentration x.

Experimental values for the linear coefficient of the specific heat γ for various refractory metal carbides and nitrides, especially VC_x and TiC_x, are given by several authors.[21–24] However, the composition of the samples is not very well defined (Caudron *et al.*[22] report deviations from the average composition of about 4%). For TiC_x, the large increase of γ with increasing vacancy concentrations is in qualitative agreement with our results. Disregarding the value given by Lowndes *et al.*[21] for $VC_{0.87}$ (which seems suspicious) their values of γ given for $VC_{0.85}$, $VC_{0.80}$, and $VC_{0.76}$ are in reasonably good agreement with ours.

Ajami and McCrone[25] calculated the density of states at the Fermi energy for VN_x from measured magnetic susceptibilities. They find, as we do, a decrease with increasing vacancy concentration. The value of the density of states at the Fermi energy for stoichiometric VN we find (25.68 states/cell Ry) agrees fairly well with the value calculated by Papaconstantopoulos *et al.*[26] (30.48 states/cell Ry), and even better with the experimental γ value quoted by Papaconstantopoulos *et al.*[26] A recent measurement of nearly stoichiometric VN (Ref. 27) yields 4.59 $mJ\,mol^{-1}\,K^{-2}$ (26.5 states/cell Ry) which is in excellent agreement with our results.

Experimental evidence of the vacancy peak is also given by photoemission measurements. Recently Bringans and

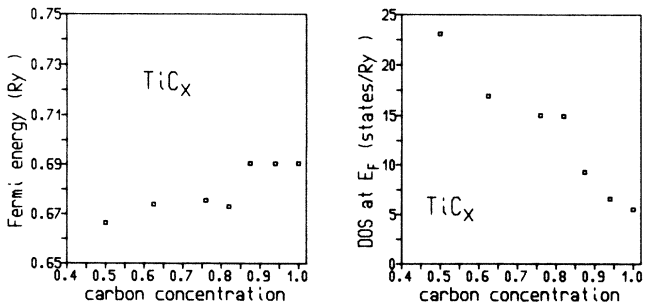

FIG. 9. Fermi energy and density of states at the Fermi energy for TiC_x versus concentration x.

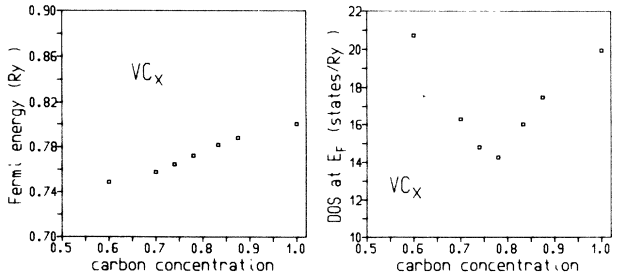

FIG. 11. Fermi energy and density of states at the Fermi energy for VC_x versus concentration x.

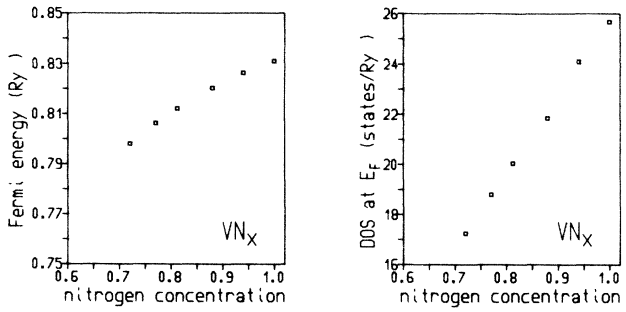

FIG. 12. Fermi energy and density of states at the Fermi energy for VN_x versus concentration x.

Höchst[28] reported a "vacancy state" about 2 eV below the Fermi level in $TiN_{0.80}$, which does not appear in $TiN_{0.99}$.

Additional vacancy states are also found by Redinger *et al.*[6] in their APW calculation of the ordered superstructure $Ti_4C_3\square$. However, there are significant differences to the present results. The sharp peaks in the density of states which in the CPA calculation are smoothed by the averaging over the configurations are retained. They find two vacancy peaks, one below and one above the Fermi energy. The second peak is of mainly p character, whereas in our calculation there are two s-like peaks, and only minor p-like contributions.

An equivalent calculation for $Ti_4N_3\square$ (Ref. 14) showed qualitatively the same behavior, except for the second vacancy peak, which now lies exactly at the Fermi energy, which would imply a tremendous increase of γ as compared to the stoichiometric compound.

The failure of the tight-binding CPA method[4,5] to detect a vacancy peak was already discussed by Klima *et al.*[7] It seems, therefore, unnecessary to repeat their arguments.

V. CONCLUSION

The appearance of vacancy peaks is a common feature of all the substoichiometric refractory metal compounds investigated. Photoemission measurements and—though not many reliable experimental values are available—specific-heat measurements generally confirm our results. We believe the KKR-CPA method yields a fairly accurate description of these systems, where other methods have completely failed, or—in the case of supercell calculations—brings about several artifacts due to the long-range order assumed.

ACKNOWLEDGMENTS

We would like to thank Dr. G. Schadler for his collaboration. Some of us (A.N. and P.W.) gratefully acknowledge partial financial support by Hochschuljubiläumsstiftung der Stadt Wien.

[1]A. Neckel, Int. J. Quatum Chem. **23**, 1317 (1983).
[2]K. Schwarz and N. Rösch, J. Phys. C **9**, L435 (1976).
[3]G. Ries and H. Winter, J. Phys. F **10**, 1 (1980).
[4]J. Klima, J. Phys. C **12**, 3961 (1979).
[5]B. Klein, D. Papaconstantopoulos, and L. Boyer, Phys. Rev. B **22**, 1946 (1980).
[6]J. Redinger, R. Eibler, P. Herzig, A. Neckel, R. Podloucky, and E. Wimmer, J. Phys. Chem. Solids **46**, 383 (1985).
[7]J. Klima, G. Schadler, P. Weinberger, and A. Neckel, J. Phys. F **15**, 1307 (1985).
[8]J. P. Landesman, thèse, Université Louis Pasteur, Strasbourg (1985).
[9]V. Moisy-Maurice, C. H. de Novion, A. N. Christensen, and W. Just, Solid State Commun. **39**, 661 (1981).
[10]M. Sauvage, E. Parthé, and W. B. Yelon, Acta Crystallogr. A **30**, 597 (1974).
[11]G. M. Stocks, W. M. Temmerman, and B. L. Györffy, *Electrons in Disordered Metals and at Metallic Surfaces,* Vol. 42 of *NATO ASI Series B,* edited by P. Phariseau *et al.* (Plenum, New York, 1979).
[12]S. Faulkner, Prog. Mater. Sci. **27**, 1 (1982).
[13]A. Neckel, P. Rastl, R. Eibler, P. Weinberger, and K. Schwarz, J. Phys. C **9**, 579 (1976).
[14]P. Herzig, J. Redinger, R. Eibler, and A. Neckel (to be published).
[15]R. E. Watson, Phys. Rev. **111**, 1108 (1958).
[16]E. Rudy, U. S. Air Force Materials Laboratory Technical Report No. AFML-TR-65-2, Part V, 1969 (unpublished).
[17]A. Nørlund Christensen and S. Fregerslev, Acta Chem. Scand. Ser. A **31**, 861 (1977).
[18]G. Brauer and W. D. Schnell, J. Less-Common Met. **6**, 326 (1964).
[19]A. Bansil, Solid State Commun. **16**, 885 (1975).
[20]W. R. Fehlner and S. H. Vosko, Can. J. Phys. **54**, 2159 (1976).
[21]D. H. Lowndes, L. Finegold, and R. G. Lye, Philos. Mag. **21**, 245 (1970).
[22]R. Caudron, J. Castaing, and P. Costa, Solid State Commun. **8**, 621 (1970).
[23]L. E. Toth, *Transition Metal Carbides and Nitrides* (Academic, New York 1971), pp. 106–107.
[24]M. Ishikawa and L. E. Toth, Monatsh. Chem. **103**, 492 (1972).
[25]F. I. Ajami and R. K. McCrone, J. Phys. Chem. Solids **36**, 7 (1975).
[26]D. A. Papaconstantopoulos, W. E. Pickett, B. M. Klein, and L. L. Boyer, Phys. Rev. B **31**, 752 (1985).
[27]C. Geibel, H. Rietschel, A. Junod, M. Pelizzone, and J. Muller, J. Phys. F **15**, 405 (1985).
[28]R. D. Bringans and H. Höchst, Phys. Rev. B **30**, 5416 (1984).